GEMP-543

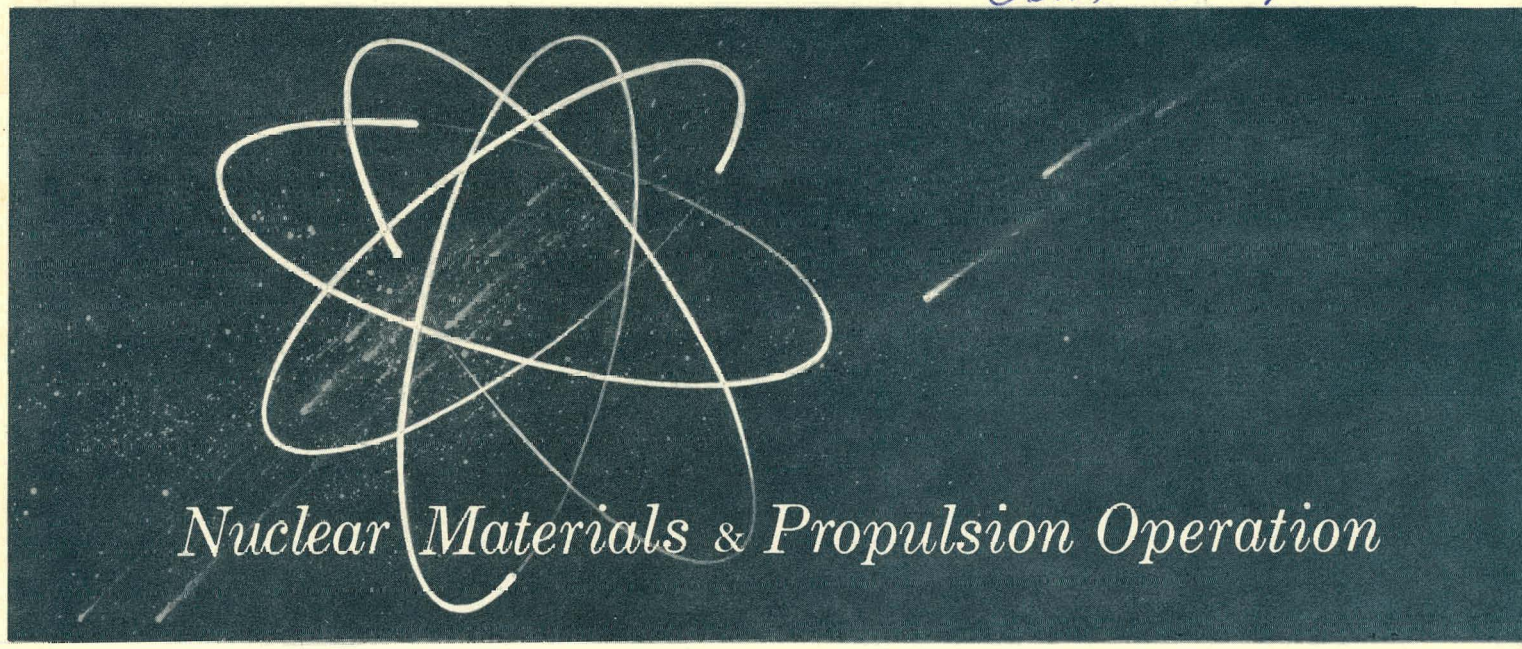

HIGH TEMPERATURE CREEP-RUPTURE BEHAVIOR OF UNALLOYED TUNGSTEN

P. N. Flagella

August 31, 1967

Presented at Third International Symposium – High Temperature Technology, Stanford Research Institute, Asilomar, California, September, 1967

NUCLEAR TECHNOLOGY DEPARTMENT
NUCLEAR ENERGY DIVISION
GENERAL ELECTRIC

DISCLAIMER

GEMP-543

HIGH TEMPERATURE CREEP-RUPTURE BEHAVIOR OF UNALLOYED TUNGSTEN

P. N. Flagella

August 31, 1967

Presented at Third International Symposium – High Temperature Technology, Stanford Research Institute, Asilomar, California, September, 1967

Work described in this paper was performed under AEC Contract AT(40-1)-2847

Nuclear Materials and Propulsion Operation
Nuclear Technology Department
Nuclear Energy Division
Cincinnati, Ohio 45215

HIGH-TEMPERATURE CREEP-RUPTURE BEHAVIOR OF UNALLOYED TUNGSTEN

by P. N. Flagella

INTRODUCTION

The use of tungsten as a structural material for engineering systems is relatively new. Since it has the highest melting point (3410°C) of all metals, it should retain useful strength at very high temperatures. Green[1] has shown this to be the case for wrought powder-metallurgy tungsten rod with short-time creep-rupture tests in the 2250° to 2800°C temperature range. The stress-rupture results of the same form of tungsten, obtained by Pugh,[2] were similar in the temperature range of 870° to 1205°C for test times approaching 400 hours. The present study observes the effect of fabrication processing on the high-temperature strength of tungsten and hence the stress-rupture, creep and ductility of unalloyed tungsten for the temperature interval of 1600° to 3000°C.

MATERIAL TESTED

Unalloyed tungsten used in this evaluation was in sheet form either 0.02 or 0.06 inch thick. The material was obtained from four different vendors; three of them supplied wrought powder-metallurgy tungsten (0.02" thick) and the fourth supplied wrought arc-cast tungsten (0.06" thick). Information on each source of material is given in Table 1. The designations W(1), W(2), and W(4) relate to the three powder-metallurgy sources; W(3) relates to the arc-cast source. The chemical analysis data in Table 1 were obtained for the as-received sheet after fabricating the material into test samples. The analysis

shows that the carbon content for the arc-cast material is two to three times that of the powder-metallurgy materials. Spectrographic analysis showed that impurity elements were not detected; they existed in "trace" amounts.

Microstructures for the as-received materials showed a wrought fibrous structure in all cases with no detectable amount of recrystallization. No additional work or heat treatment was performed on any of the materials before testing.

TEST SPECIMEN

All creep-rupture specimens were cut from the sheets using the electrical discharge machining (EDM) technique. The stress axes of the specimens were in the major rolling direction of each sheet. Approximately 0.02 inch of material was then removed from the specimen gage section width by low-stress surface grinding. The specimen gage section was 0.25 inch wide and 1.00 inch long with a fillet of 0.25-inch radius at each end. Overall length and width of the specimens were 3.0 inches and 0.75 inch, respectively, with 0.25-inch holes located at each end for pin connections to the load train.

TESTING PROCEDURE

The constant-load creep-rupture testing equipment has been previously reported.[3] The test specimen is suspended from the top of the furnace pressure shell and located in the center of a tungsten split-tube heating element. The lower load-train is suspended from the specimen and is used for dead weight loading. Both the load-train assembly and weights are in the furnace shell; loading is performed by actuating a vertical push rod ("O" ring sealed) through the bottom of the shell. The test specimen is heated by thermal radiation from the resistively-heated tungsten heating element. During the creep-rupture testing, the specimen temperature was maintained constant to within $\pm 5^{\circ}C$ by automatically maintaining a constant

heating element voltage. Most tests were performed in a hydrogen atmosphere slightly above atmospheric pressure. For comparison, some tests were performed in argon at the same pressure. Specimen temperature was established with an L. and N. optical pyrometer having a calibration traceable to N.B.S. A black-body target, located beside the specimen, in the form of a .03-inch hole drilled through one wall of a .125-inch diameter by .75-inch long closed end tungsten tube, permitted accurate temperature measurements without specimen emissivity corrections. Furnace sight glass (quartz) absorption corrections were based on experimental measurements at the temperatures involved.

During the initial phase of this study, the creep-strain measurements were based on the elongation of the total train. The measurements were consistent for comparisons but they were not precise, since creep of the fillets and pin holes was included. All creep data for the three powder-metallurgy materials were obtained in this manner.

Before testing the arc-cast material, a technique was developed to obtain accurate creep-strain measurements. A twin-scope optical extensometer was used to sight through the furnace window on the side of the pressure shell. The vertical slots of the split-tube heating element and the matching slots in the radiation shields permitted sighting onto the sample fiducial marks (0.005-inch diameter holes) at each end of the specimen gage length.

After the specimen was installed the test chamber was sealed and evacuated; furnace walls were outgassed by circulating hot water through the cooling passages. The specimen was then heated to approximately 1100^{o}C and the chamber was filled with the test gas atmosphere. Heating was resumed for about 15 minutes, until desired test temperature was attained. Annealing of all specimens was performed at the test temperature for two hours before the load was applied.

RESULTS

The stress-rupture and creep rate test results for the four different sources of tungsten sheet are given in Tables 2 through 5. Figure 1 shows the stress-rupture data for each material. Available data indicate significant differences in the time-to-rupture for the same temperature and stress, although each material was not tested over the total temperature range. In all cases the arc-cast material, W(3), had the shortest time to rupture even though the elongation at rupture was considerably greater at all temperatures. This indicates that the arc-cast material is less creep resistant and more ductile than any of the powder-metallurgy materials. The differences in the rupture life are greatest at the higher temperatures. One apparent reason for the differences noted is the grain-size effect. After test, the powder-metallurgy materials were usually fine grained; some duplexing was observed, however, at the higher temperatures. The arc-cast material contained large grains at the lower temperatures which became so huge at the higher temperatures that they encompassed the total cross section of the specimen. Considerable substructure with low-angle boundaries was observed in the arc-cast material whereas none was apparent in the powder-metallurgy materials.

With the exception of the W(4) powder-metallurgy material at 2600°C, the stress-rupture results obtained in hydrogen or argon atmospheres were essentially the same for the same material within the scatter of the experimental data.

The ductility of the arc-cast material was greater than that of the powder-metallurgy material, as mentioned earlier. Figure 2 shows how the ductility of the two materials, based on the elongation at rupture, varied with temperature. Although the bands are relatively broad for both forms of material, the arc-cast tungsten shows a peak in ductility in the 2200° to 2400°C region; the

ductility of the powder-metallurgy tungsten decreases with increasing temperature over the total temperature range investigated.

The method of deformation and fracture was quite different for the two forms of material. The powder-metallurgy material, as noted, was mostly fine grained with randomly dispersed large grains in specimens tested at the higher temperatures and longer test times. Despite the large grains, fracture always occurred at the grain boundaries as the result of intergranular cavities forming and linking up at boundaries perpendicular to the stress direction. On the other hand, the arc-cast material contained large grains even at the lower temperatures and after short test times. No grain-boundary separation was observed over the total temperature range and most of the deformation appeared to occur intragranularly, except for that due to grain boundary sliding. The actual mode of fracture was difficult to determine but appeared to be intragranular after considerable area reduction within the large grains. Typical microstructures are shown in Figure 3.

A previous study[4] of the stress-rupture characteristics of unalloyed molybdenum showed that the results obtained from various sources of wrought arc-cast sheet were essentially the same; wrought powder-metallurgy materials were not. Extending this conclusion to the results obtained for tungsten indicates that the data for arc-cast tungsten are more representative of the material and not influenced by processing history, at least above one-half the absolute melting temperature. This is somewhat substantiated by combining the stress-rupture data of arc-cast molybdenum, mentioned above, with the arc-cast tungsten data from this study. Consistent behavior is observed on a homologous temperature isochronal plot as shown in Figure 4. In addition to being linear on a log-stress versus homologous-temperature plot, the data

corresponding to rupture in a given time are coincident for these two Group VI-A metals. Pugh[2] compared the tensile strengths of recrystallized tungsten, molybdenum, and chromium using the homologous temperature scale with good agreement, indicating that Figure 4 may also apply to chromium. Furthermore, since tungsten and molybdenum form solid solutions over the complete range of binary phase diagram, Figure 3 may apply to any of the alloys of tungsten and molybdenum. Experimental investigations are required to substantiate this. A further possibility is that the same curves may apply to any alloys involving the three metals so long as they are in solution.

Figure 5 shows the stress versus linear creep rate (secondary) data given in Table 2 on the basis of constant temperature. The curves are consistent with those in Figure 1: data vary for each source of material at the same test conditions. The arc-cast material is the least creep resistant even though the data for the powder-metallurgy materials are based on "total train" elongations. The test results given in Tables 3 and 4 show some values of creep rate for both "total train" and 1-inch gage section. In each case the gage section data give lower values of creep rate.

The steady-state creep-rate data for the arc-cast tungsten from 1600° to 3000°C were evaluated based on the proposed method of Sherby[5] for pure polycrystalline metals above one-half the absolute melting temperature. The results are presented in Figure 6 in terms of the ratio of steady-state creep rate ($\dot{\varepsilon}$) to the diffusion coefficient (D) plotted as a function of the creep stress (σ) divided by the elastic modulus (E). The values for diffusion coefficient[6] and elastic modulus[7] were obtained from the literature. Correlation of the data in this manner appears to be quite good, with the same curve shape as that determined by Sherby for other pure polycrystalline metals.

The slope (n) of the linear portion of the curve was calculated to be 4.2 and is consistent with the Sherby prediction that the value for n should be approximately 5. This portion of the curve is associated with the creep process controlled by dislocation climb involving an equilibrium vacancy concentration. The nonlinear portion of the curve (high stresses) involves the dislocation climb creep under conditions in which the vacancy concentration is greater than the equilibrium number.

Based on creep data obtained from arc-cast tungsten in the temperature range of 2200° to 2800°C, an analysis was made of the equation forms available for expressing the first stage creep behavior. Least squares computer programs were developed to obtain unique solutions for all the constants of the creep equations. Table 6 lists the equation forms used, with a typical comparison of the effectiveness of the equations for data at 2400°C and 1,000 psi. All the equations studied express the test data very well as indicated by the values for the standard deviation, δ. Most effective, however, are the polynomial in $t^{1/3}$, the hyperbolic sine[8] equation and the de Lacombe[9] equation. Less effective were the Cottrell-Aytekin[10] equation, the Andrade[11] equation using an exponent of 1/3, and the parabolic equation. Examples of the effectiveness of the equations used in this study are presented in Figure 7 for the arc-cast tungsten data at 2400°C and 1,200 psi. In each case the solid curves were calculated using the equation forms given in Table 6. The agreement with the experimental points is excellent. Similar results were obtained for the other stresses and temperatures evaluated. The first stage creep behavior of unalloyed arc-cast tungsten, to at least 85 percent of the absolute melting temperature, can apparently be represented by equation forms developed from the creep data of metals having much lower melting temperatures.

SUMMARY

Unalloyed wrought arc-cast tungsten sheet exhibits a shorter rupture life, is less creep resistant, and is considerably more ductile than unalloyed wrought powder-metallurgy tungsten sheet for the temperature range of 1600° to 3000°C. Considerable variation in the creep-rupture behavior was observed in the wrought-powder-metallurgy tungsten from various vendors. This observation is the same as that made in a previous investigation for molybdenum. In a comparison of the rupture data for arc-cast tungsten and arc-cast molybdenum on a homologous temperature isochronal plot, consistent behavior is shown. The data for the two materials are coincident on a log-stress versus homologous-temperature plot.

Steady-state creep data for the arc-cast tungsten show a good correlation when corrections for elastic modulus and diffusion coefficient are applied.

Analysis of the transient creep process of arc-cast tungsten was made using various first-stage creep equations. Experimental data were best described using a polynomial in $t^{1/3}$, the de Lacombe equation, and a hyperbolic sine creep equation. Several other equation forms, including the Anbrade and Cottrell-Aytekin equations, are also fairly accurate.

ACKNOWLEDGEMENTS

Credit is due to W. L. McCullough and J. H. Foster for developing the experimental equipment and techniques, and for performing the tests. The financial support of the Fuels and Materials Branch, Division of Reactor Development and Technology of the U.S. Atomic Energy Commission, is gratefully acknowledged.

REFERENCES

1. Green, W. V., "Short Time Creep-Rupture Behavior of Tungsten at 2250° to 2800°C," Trans. AIME, Vol. 215, 1959, p. 1057.
2. Pugh, J. W. "Tensile and Creep Properties of Tungsten at Elevated Temperatures," ASTM, Vol. 57, 1957, p. 906.
3. McCullough, W. L., Flagella, P. N., "Experimental Techniques Employed in Stress-Rupture and Creep Measurements to 3000°C," GE-NMPO, GE-TM 65-5-10, April 1965.
4. Flagella, P. N., "High Temperature Stress-Rupture Characteristics of Mo and Some Mo Alloys," AIAA Journal, Vol. 2, No. 2, Feb. 1967, p. 281.
5. Sherby, O. D., "Factors Affecting the High-Temperature Strength of Polycrystalline Solids," Acta Metallurgica, Vol. 10, Feb 1962, p. 135.
6. Dannerberg, W., Metall., Vol. 15, 1961, p. 977.
7. Armstrong, P. E., Brown, H. L., "Dynamic Young's Modulus Measurements Above 1000°C on Some Pure Polycrystalline Metals and Commercial Graphites," Metal. Soc. of AIME, Vol. 230, July-Dec. 1964, p. 962.
8. Conway, J. B., Mullikin, M. J., "An Evaluation of Various Equations for Expressing First-Stage Creep Behavior," Trans AIME, Vol. 236, Oct. 1966, p. 1496
9. de Lacombe, J., "A Method of Representing Creep Curves," Rev. Metal., Vol. 36, 1939, p. 178.
10. Cottrell, A. H., Aytekin, V., "Andrade's Creep Law and the Flow of Zink Crystals," Nature, Vol. 160, 1947, p. 328.
11. Andrade, E. N. da C., "On the Viscous Flow in Metals and Allied Phenomena," Proceedings of the Royal Society, Vol. 84, 1910, p. 1.

TABLE 1

PROCESSING AND ANALYSIS DATA FOR TUNGSTEN

	W(1)	W(2)	W(3)	W(4)
Source	Commercial	Commercial	RMSRP[a]	RMSRP[b]
Processing[c]	PM	PM	AC	PM
Sintering Temp, °C	?	?	melt	2300
Reduction	?	d	e	f
Sheet Thickness, inches	0.02	0.02	0.06	0.02
Sheet Size, inches	0.9 x 7.5	4.7 x 24	13.5 x 21.5	14.1 x 29.5
Analysis, ppm				
C	18	18	63	28
O	38	32	5.6	10
H	4	2	0.7	2
N	3	3	0.1	0.8

[a]Refractory Metals Sheet Rolling Program, U.S. Navy, Contract No. NOw-60-0621-c.
[b]Refractory Metals Sheet Rolling Program, U.S. Air Force, Contract No. AF 33(600)-41917.
[c]PM, wrought powder-metallurgy.
AC, wrought arc-cast.
[d]Approximately 25 reductions from forged ingot to final thickness.
[e]After recrystallization – 92 to 94%. After stress relief – 80 to 85%.
[f]73% warm worked.

TABLE 2

CREEP-RUPTURE RESULTS[a] FOR WROUGHT POWDER METALLURGY TUNGSTEN SHEET[b] W(1)

Specimen No.	Atm	Temperature, °C	Stress, psi	Rupture Time, hr	Rupture Strain, %	Linear Creep Rate, min^{-1} Total Train	Linear Creep Rate, min^{-1} 1" Gage Length
1	H_2	1600	11,000	1.84	41	2.2×10^{-3}	
2	H_2	1600	11,000	2.70	43	1.6×10^{-3}	
3	H_2	1600	10,000	6.06	40	5.0×10^{-4}	
4	H_2	1600	9,500	11.14	38	3.3×10^{-4}	
6	H_2	1600	12,000	1.85	48	2.6×10^{-3}	
8	H_2	1600	13,000	1.06	55	4.0×10^{-3}	
19	H_2	1600	10,000	8.37	46	5.9×10^{-4}	
7	H_2	1600	10,000	6.0	42	6.0×10^{-4}	
28	A	2800	1,500	.154	26		
26	A	2800	1,200	.75	10	4.0×10^{-4}	
27	H_2	2800	1,000	11.0	0	3.36×10^{-5}	
29	H_2	2800	1,200	2.15	14	–	
25	H_2	2800	1,200	1.70	4	5.56×10^{-4}	

[a]Annealed for 2 hours at test temperature in H_2 prior to test.

[b]0.02 inches thick, 0.25 inches x 1.00 inch gage section.

TABLE 3

CREEP-RUPTURE RESULTS[a] FOR WROUGHT POWDER METALLURGY TUNGSTEN SHEET[b] W(2)

Specimen No.	Atm	Temperature, °C	Stress, psi	Rupture Time, hr	Rupture Strain, %	Linear Creep Rate, min^{-1} Total Train	Linear Creep Rate, min^{-1} 1" Gage Length
7	H_2	1600	8,000	19.48	70	2.8×10^{-4}	
11	H_2	2000	3,000	5.74	41	1.7×10^{-4}	1.2×10^{-4}
8	H_2	2000	3,000	5.16	33	2.6×10^{-4}	1.7×10^{-4}
34	H_2	2200	2,000	6.27	30	5.2×10^{-4}	
35	A	2200	2,000	2.82	35	2.1×10^{-4}	
33	H_2	2200	2,200	4.18	20	5.6×10^{-4}	
31	H_2	2200	2,600	1.30	24	2.9×10^{-3}	
32	A	2200	2,600	.99	30	4.0×10^{-3}	
37	H_2	2200	2,400	2.15	26	1.2×10^{-3}	
38	A	2200	1,800	9.31	14	7.9×10^{-5}	
36	H_2	2200	1,800	14.25	23	1.8×10^{-4}	
44	H_2	2200	1,600	33.83	25	8.5×10^{-5}	
42	H_2	2200	1,300	189.5	21	1.3×10^{-5}	
11	H_2	2400	1,600	2.82	26	1.0×10^{-3}	
12	H_2	2400	1,400	6.08	21	4.4×10^{-4}	
13	H_2	2400	1,900	1.22	28	2.6×10^{-3}	
15	H_2	2400	1,200	11.67	16	1.7×10^{-4}	
14	H_2	2400	2,100	.94	26	3.4×10^{-3}	
16	H_2	2400	2,500	.43	32	8.7×10^{-3}	
8	A	2400	1,600	1.56	18	1.3×10^{-3}	
17	H_2	2400	1,600	2.00	16	9.8×10^{-4}	
10	H_2	2400	1,500	4.22	25	6.2×10^{-4}	5.3×10^{-4}
18	A	2400	1,400	2.30	14	6.2×10^{-4}	
20	A	2400	2,000	.54	24	3.5×10^{-3}	
21	H_2	2400	958	37.5	10	3.0×10^{-5}	
22	A	2400	1,000	23.02	5	2.7×10^{-5}	
27	A	2400	1,500	5.26	14	2.4×10^{-4}	
26	H_2	2400	1,500	3.42	16	3.9×10^{-4}	
28	A	2400	1,500	3.84	18	4.3×10^{-4}	
29	A	2400	1,500	3.83	12	3.6×10^{-4}	
1	H_2	2800	1,200	.42	22	5.3×10^{-3}	
2	H_2	2800	1,200	.65	28	4.4×10^{-3}	
4	H_2	2800	1,000	1.65	31	2.0×10^{-3}	
3	A	2800	1,200	.45	32	7.4×10^{-3}	
5	A	2800	1,000	1.65	22	–	
6	A	2800	800	7.61	16	–	
7	A	2800	900	2.65	20	5.8×10^{-4}	
10	H_2	2800	550	62.25	12	1.7×10^{-5}	
9	H_2	2800	650	39.75	7	2.4×10^{-5}	
19	H_2	2800	900	3.18	18	5.0×10^{-4}	
23	H_2	2800	500	94.45	9	1.0×10^{-5}	

[a]Annealed for 2 hours at test temperature in H_2 prior to test.
[b]0.02 inches thick, 0.25 inches x 1.00 inch gage section.

TABLE 4

CREEP-RUPTURE RESULTS[a] FOR WROUGHT POWDER METALLURGY TUNGSTEN SHEET[b] W(4)

Specimen No.	Atm	Temperature, °C	Stress, psi	Rupture Time, hr	Rupture Strain, %	Linear Creep Rate, min^{-1} Total Train	Linear Creep Rate, min^{-1} 1" Gage Length
76	H_2	1600	10,000	2.48	62	2.1×10^{-3}	1.7×10^{-3}
64	H_2	1600	8,600	5.91	34	5.7×10^{-4}	4.5×10^{-4}
68	H_2	1600	10,000	2.40	40	1.6×10^{-3}	1.3×10^{-3}
70	H_2	1600	7,800	9.25	44	4.4×10^{-4}	3.8×10^{-4}
71	H_2	1600	5,000	5.2[c]			
73	H_2	1600	6,000	51.27	32	5.4×10^{-5}	4.4×10^{-5}
75	H_2	1600	8,000	9.47	34	3.9×10^{-4}	3.0×10^{-4}
79	H_2	2000	3,000	23.17	27	8.8×10^{-5}	6.3×10^{-5}
10	H_2	2200	1,600	60.65	17	3.6×10^{-5}	
16	H_2	2200	2,500	4.18	44	2.1×10^{-3}	
21	H_2	2200	3,000	2.10	27	1.1×10^{-3}	
18	H_2	2200	2,000	15.3	15	1.2×10^{-4}	
24	H_2	2200	2,500	4.94	22	3.8×10^{-4}	
22	A	2200	2,500	6.64	31	3.5×10^{-4}	
56	A	2200	3,000	1.44	64	6.7×10^{-4}	
60	H_2	2200	3,000	3.15	26	6.3×10^{-4}	
61	H_2	2200	2,905	1.3	39	—	
25	H_2	2200	1,600	20.5[a]	3.2	—	
72	H_2	2400	1,500	7.62	29	2.5×10^{-4}	1.9×10^{-4}
7	H_2	2600	1,000	25.08	5	1.5×10^{-5}	
8	H_2	2600	1,200	8.84	8	9.1×10^{-5}	
9	H_2	2600	1,400	3.50	12	3.9×10^{-4}	
11	H_2	2600	1,700	.82	20	2.0×10^{-3}	
12	A	2600	1,400	.41	12	2.5×10^{-3}	
13	A	2600	1,000	4.61	8	4.0×10^{-5}	
15	A	2600	1,300	3.65	4	1.9×10^{-4}	

[a]Annealed for 2 hours at test temperature in H_2 prior to test.
[b]0.02 inches thick, 0.25 inches x 1.00 inch gage section.
[c]No rupture, test terminated.

TABLE 5

CREEP-RUPTURE[a] RESULTS FOR WROUGHT ARC-CAST TUNGSTEN SHEET[b] W(3) IN HYDROGEN

Specimen No.	Temperature, °C	Stress, psi	Time to Indicated Strain, hr							Rupture		Linear Creep Rate, min^{-1} 1" Gage Length
			0.2%	0.5%	1%	2%	3%	5%	10%	Time, hr	Strain, %	
69	1600	8,000	–	–	0.07	0.32	0.74	1.83	3.75	6.45	73	2.9×10^{-4}
70	1600	7,000	–	0.02	0.15	0.73	1.65	4.20	7.85	14.7	65	1.3×10^{-4}
48	1600	6,000	–	0.08	0.46	2.00	4.40	10.4	16.2	30.9	76	5.1×10^{-5}
71	1600	4,800	–	0.35	2.15	8.60	18.2	40.3	64.0	160.	89	1.5×10^{-5}
47	1600	4,800	0.08	0.73	3.05	10.8	21.7	45.5	76.8	137.	c	1.4×10^{-5}
50	1800	4,800	–	0.02	0.13	0.58	1.25	2.85	4.85	7.60	60	1.9×10^{-4}
51	1800	4,000	–	0.10	0.51	2.00	4.30	9.90	14.7	28.4	73	6.1×10^{-5}
52	1800	3,000	0.05	0.75	3.00	11.5	21.7	46.0	92.2	150.	62	1.4×10^{-5}
53	2000	3,000	–	–	0.08	0.50	1.15	2.63	3.85	6.70	70	2.4×10^{-4}
58	2000	2,500	–	0.03	0.25	1.36	3.00	5.15	6.35	17.6	60	9.8×10^{-5}
39	2000	2,000	0.02	0.35	1.90	5.95	8.35	10.6	17.2	63.1	94	4.6×10^{-5}
45	2000	1,500	0.17	1.65	6.30	16.5	25.2	45.3	101.	256.	65	1.5×10^{-5}
13	2200	2,000	–	–	0.02	0.19	0.48	1.23	330	7.72	74	4.0×10^{-4}
40	2200	1,800	–	0.01	0.09	0.52	1.12	2.55	–	3.35	c	2.3×10^{-4}
14	2200	1,500	–	0.06	0.37	1.52	3.10	6.60	14.8	40.7	106	9.6×10^{-5}
15	2200	1,200	0.02	0.42	1.90	6.40	11.8	22.3	48.0	119.	86	3.1×10^{-5}
16	2200	1,000	0.12	1.33	5.20	14.5	25.0	46.5	95.0	237.	125	1.5×10^{-5}
38	2400	1,500	–	–	–	0.08	0.20	0.50	1.30	3.09	86	1.0×10^{-3}
17	2400	1,200	–	–	0.05	0.28	0.60	1.40	3.42	9.25	73	4.0×10^{-4}
21	2400	1,000	–	0.03	0.18	0.74	1.50	3.10	7.40	17.5	83	2.0×10^{-4}
24	2400	800	–	0.17	0.80	2.70	5.00	10.0	21.3	61.4	120	7.0×10^{-5}
22	2400	650	0.04	0.53	2.10	6.70	11.8	22.0	46.0	146.	102	3.3×10^{-5}
19	2600	1,200	–	–	–	–	0.025	0.086	0.24	0.78	78	5.0×10^{-3}
25	2600	800	–	–	0.02	0.12	0.27	0.65	1.62	4.77	64	8.5×10^{-4}
33	2600	650	–	0.04	0.22	0.72	1.32	2.65	5.60	15.0	104	2.6×10^{-4}
26	2600	500	0.02	0.18	0.62	2.00	3.50	6.50	13.5	43.4	87	1.1×10^{-4}
27	2600	400	0.12	0.75	2.30	6.20	10.3	19.2	41.0	123.	84	3.8×10^{-5}
28	2800	500	–	–	0.015	0.10	0.27	0.67	1.60	4.30	64	8.3×10^{-4}
29	2800	400	–	0.026	0.12	0.54	1.10	2.50	5.60	14.0	74	2.4×10^{-4}
36	2800	300	0.06	0.33	1.15	3.40	6.30	13.7	28.8	51.9	46	4.9×10^{-5}
34	2800	250	0.30	1.43	4.30	12.2	22.0	43.5	79.0	144.	40	1.5×10^{-5}
49	3000	300	–	–	0.01	0.08	0.21	0.61	1.82	2.80	22	6.7×10^{-4}

[a]Annealed for 2 hours at test temperature in H_2 prior to test.
[b]0.06 inches thick, 0.25 inches x 1.00 inch gage section.
[c]No rupture, test terminated.

TABLE 6

A COMPARISON OF THE DEGREE OF REPRESENTATION AFFORDED BY VARIOUS CREEP EQUATIONS FOR THE FIRST-STAGE CREEP DATA FOR ARC-CAST TUNGSTEN AT 2400°C AND 1,000 PSI[a]

		$\mu^b \times 10^4$
Parabolic	$\epsilon = 3.5 \times 10^{-3} + 1.42 \times 10^{-3} t^{0.64}$	2.9
Andrade	$1 + \epsilon = 1.0017 (1 + 3.0 \times 10^{-3} t^{1/3}) e^{1.604 \times 10^{-4} t}$	1.9
Cottrell-Aytekin	$\epsilon = 1.002 + 1.652 \times 10^{-4} t + 2.964 \times 10^{-3} t^{1/3}$	1.88
de Lacombe	$\epsilon = -1.61 \times 10^{-3} + 6.29 \times 10^{-3} t^{0.194} + 1.28 \times 10^{-4} t^{1.09}$	1.7
Hyperbolic Sine	$\epsilon = 1.47 \times 10^{-3} + 6.67 \times 10^{-3} \sinh 0.486\ t^{1/3}$	1.7
Polynomial	$\epsilon = 5.24 \times 10^{-4} + 4.9 \times 10^{-3} t^{1/3} - 9.03 \times 10^{-4} t^{2/3} + + 2.92 \times 10^{-4} t$	1.7

[a] t = time in minutes, ϵ = strain.

[b] μ = standard deviation.

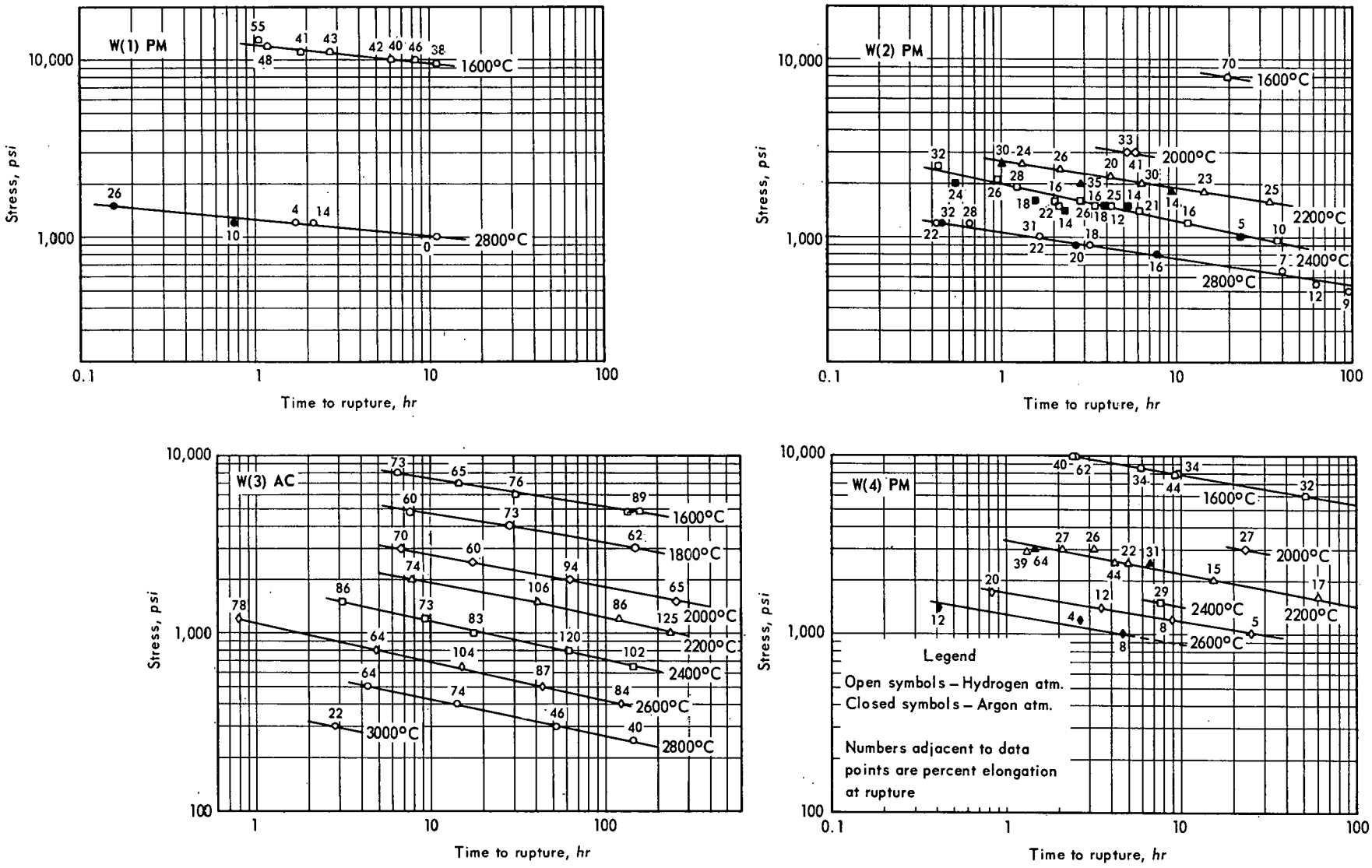

Fig. 1 – Stress-rupture results for wrought W sheet

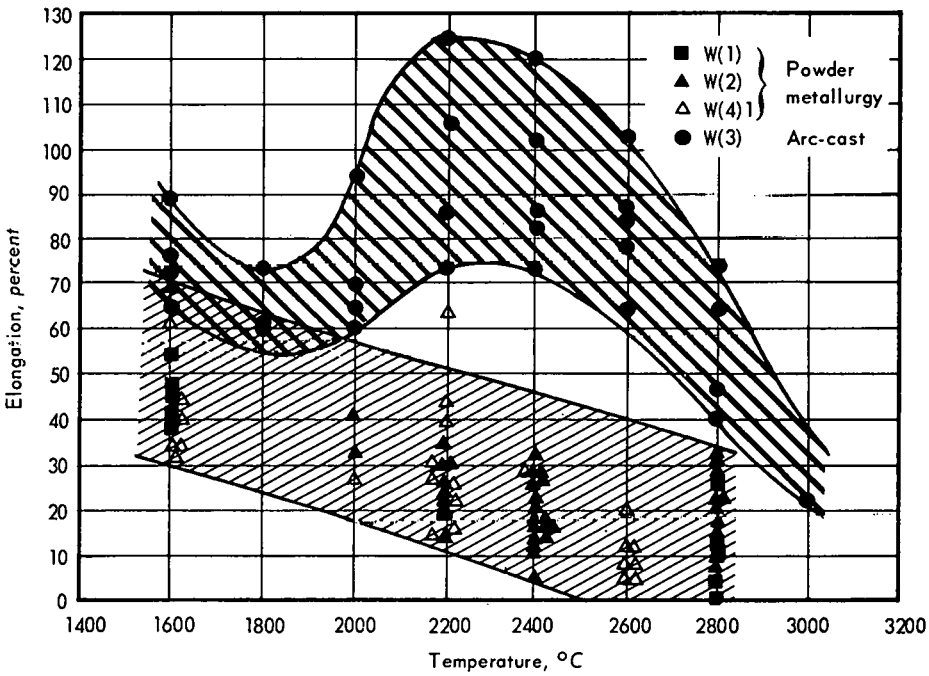

Fig. 2 – Elongation versus temperature for wrought powder-metallurgy and wrought arc-cast unalloyed W sheet tested in hydrogen

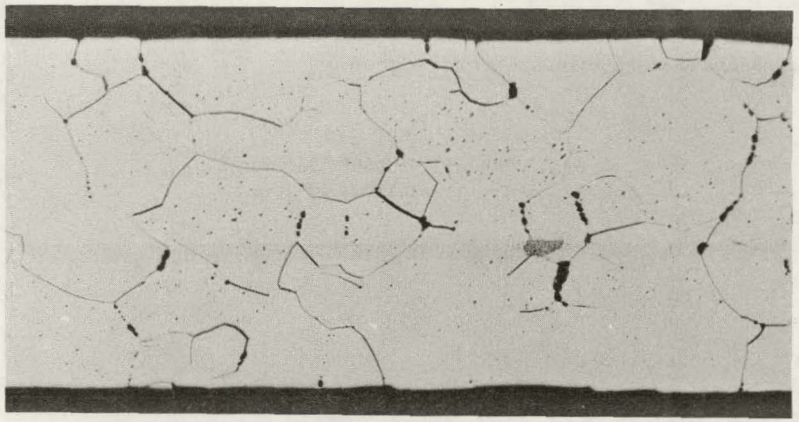

W(1)–25 powder–metallurgy
2800°C, 1200 psi, 1.7 hours, 4.2%
(Neg. 2065, 100X)

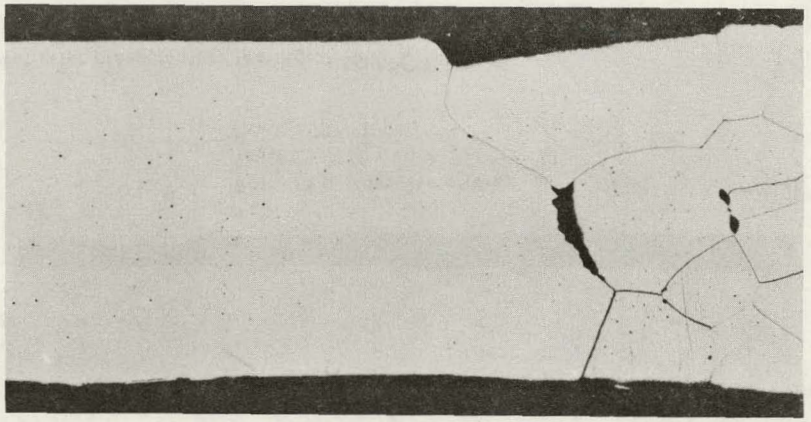

W(2)–10 powder–metallurgy
2800°C, 550 psi, 62.2 hours, 10%
(Neg. 3119, 100X)

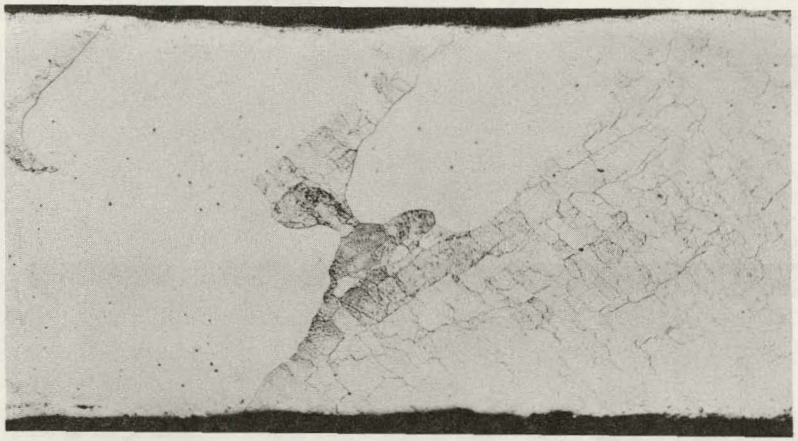

W(3)–34 arc–cast
2800°C, 250 psi, 144 hours, 40%
(Neg. 5655, 50X)

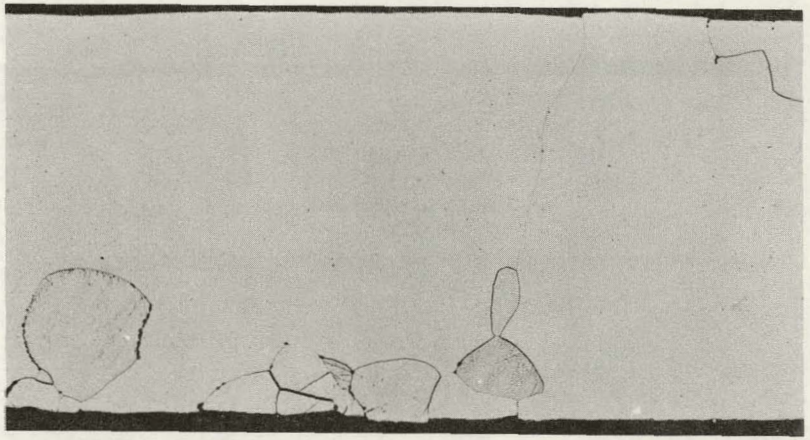

W(4)–9 powder–metallurgy
2600°C, 1400 psi, 3.5 hours, 12%
(Neg. 4140, 100X)

Fig. 3A – Typical microstructure of wrought W sheet after creep-rupture testing at 2600° and 2800°C *(etched)*

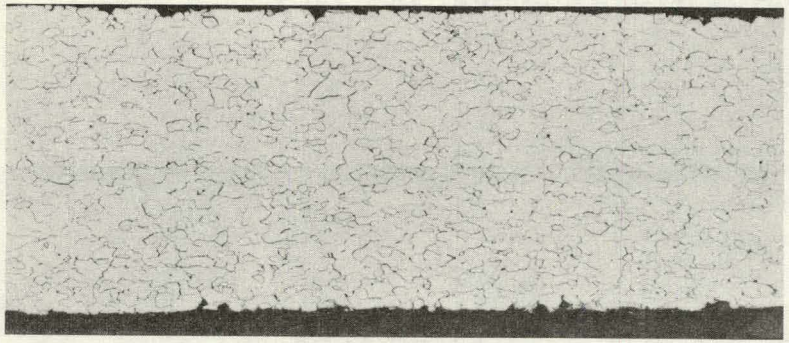

W(1)–4 powder–metallurgy
1600°C, 9500 psi, 11.1 hours, 38%
(Neg. 2006, 100X)

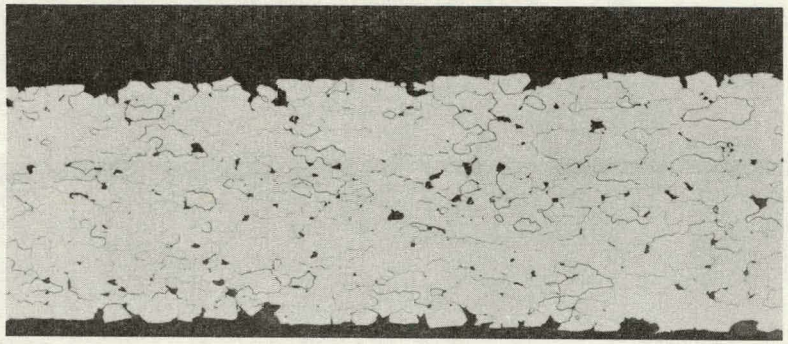

W(2)–7 powder–metallurgy
1600°C, 800 psi, 19.5 hours, 63%
(Neg. 6082, 100X)

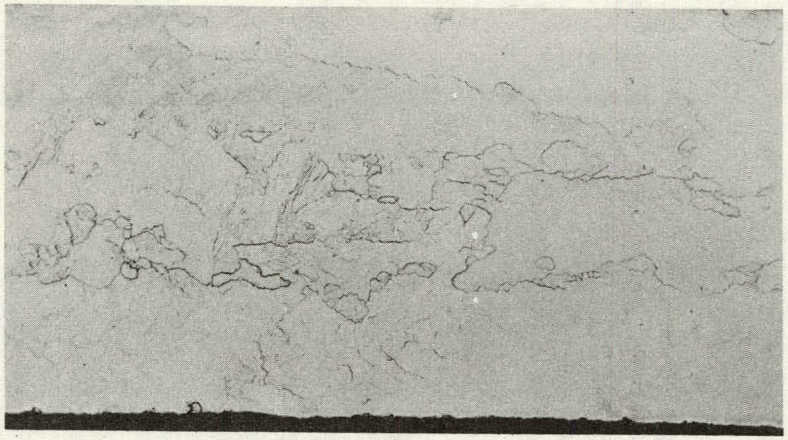

W(3)–69 arc–cast
1600°C, 8000 psi, 6.5 hours, 71%
(Neg. 6017, 50X)

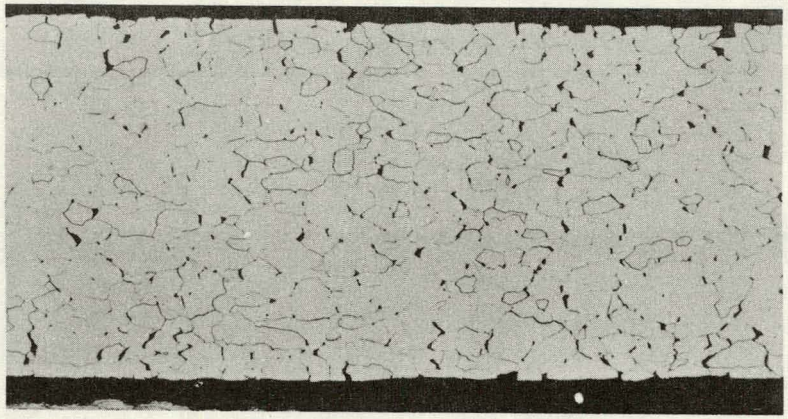

W(4)–75 powder–metallurgy
1600°C, 8000 psi, 9.5 hours, 30%
(Neg. 6081, 100X)

Fig. 3B – Typical microstructures of wrought W sheet after creep-rupture testing at 1600°C *(etched)*

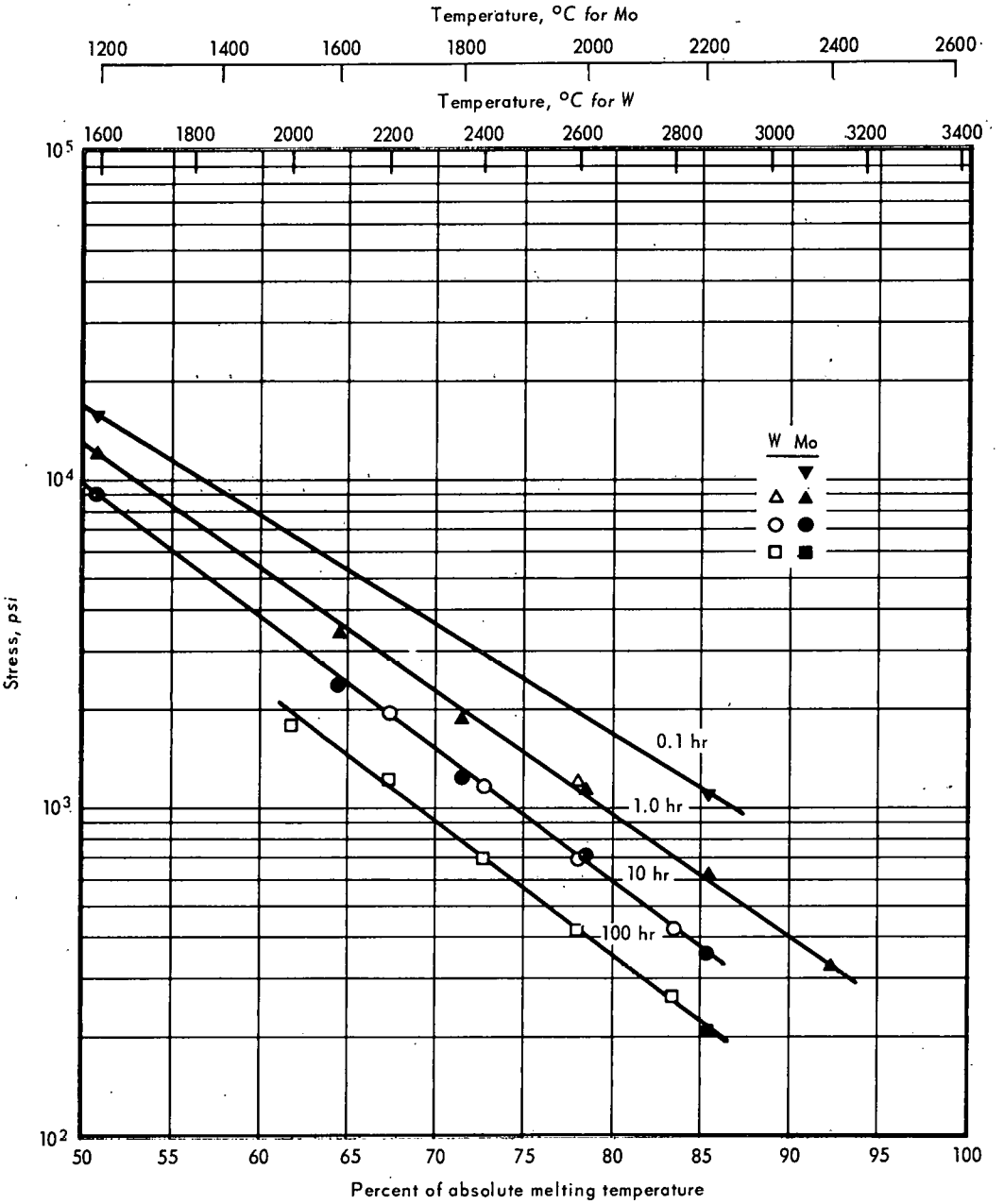

Fig. 4 – Isochronal plot of stress-rupture data for arc-cast W and Mo

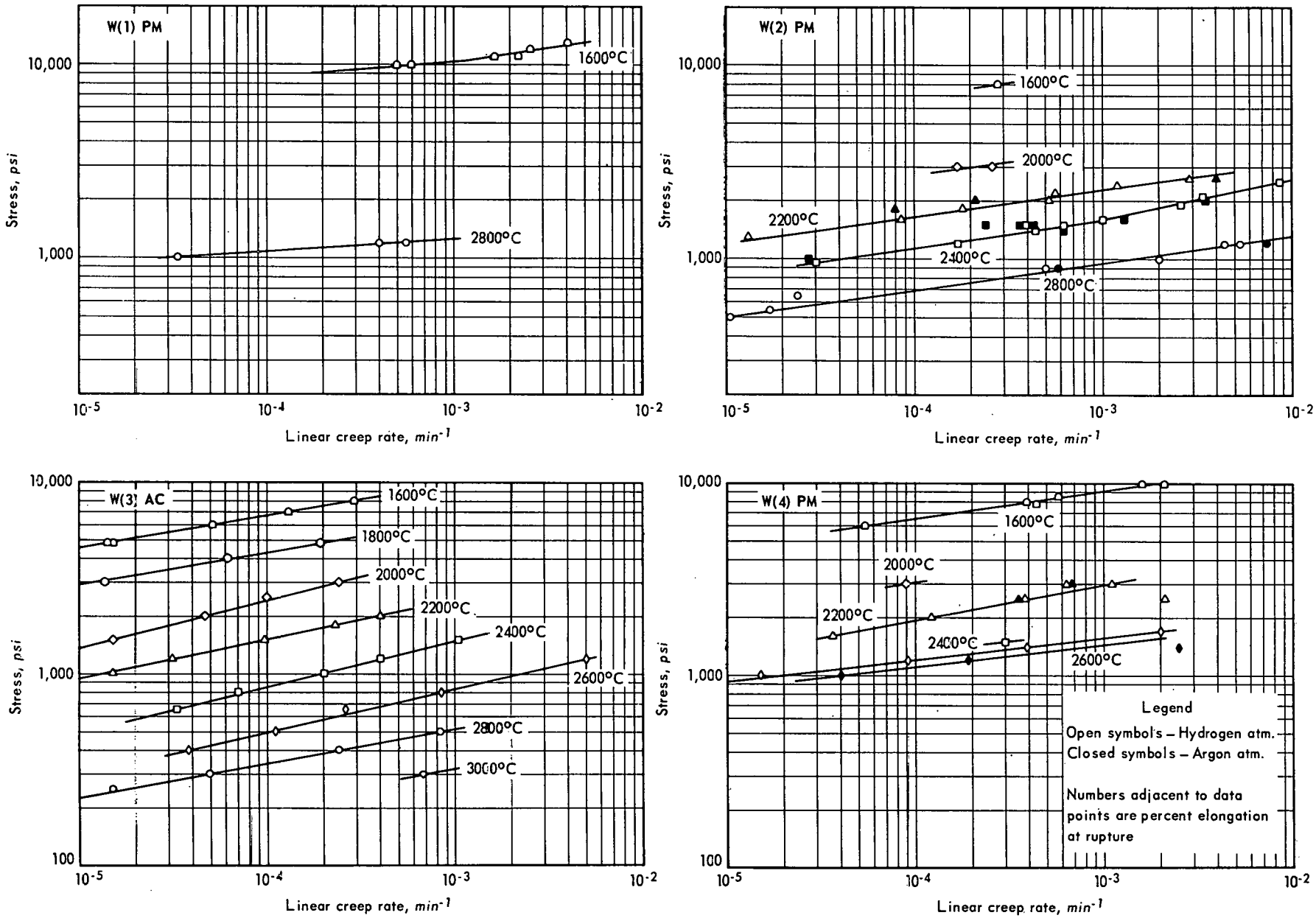

Fig. 5 – Stress versus creep rate test results for wrought W sheet

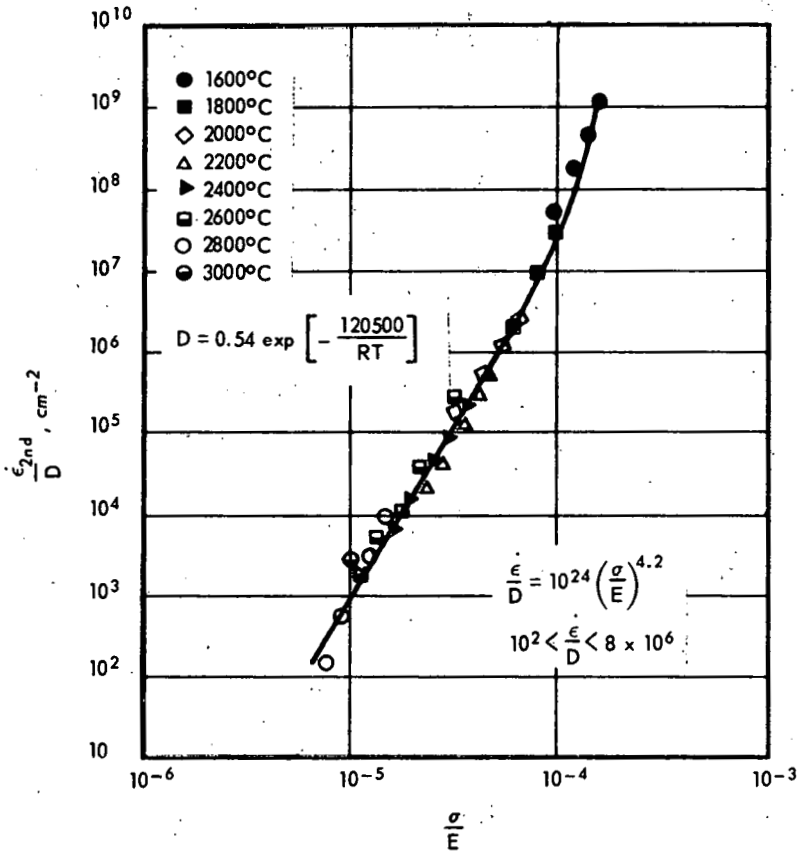

Fig. 6 – Ratio of steady-state creep rate ($\dot{\epsilon}$) to diffusion coefficient (D) versus ratio of stress (σ) to Young's modulus (E) for arc-cast W

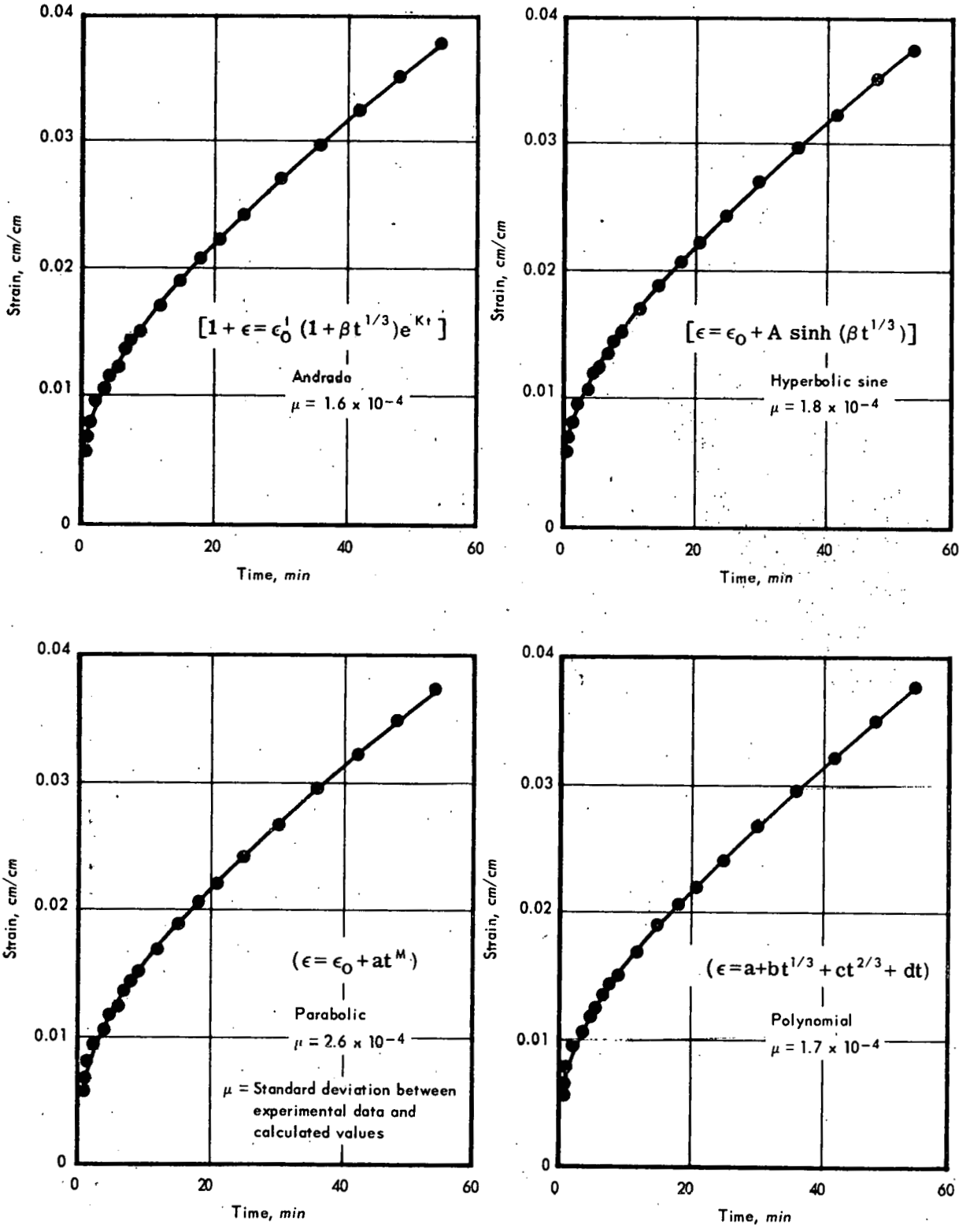

Fig. 7 – Effectiveness of various equation forms in representing data for arc-cast W at 2400°C and 1,200 psi

NUCLEAR TECHNOLOGY DEPARTMENT
NUCLEAR ENERGY DIVISION
GENERAL ELECTRIC